

Microwave Journal

Editor's Note: In Part II, the authors look at a new way to reduce stiction effects in the Resistive MEMS switch (metal-to-metal contact) using an artificial engineered structure (metamaterial). As described in Part I (May issue), the combination of a primary shunt switch, DGS structures and secondary shunt switches, is shown to behave like a metamaterial. In addition to this design, metamaterial layers within the design of the switch contacts are proposed to reduce stiction issues in the MEMS switch. Part III of this series will be published in July.

A Microelectromechanical Switch with Metamaterial Contacts: Concepts and Technology Part II



Shiban K. Koul and Chaitanya Mahajan
C.A.R.E, Indian Institute of Technology, Delhi, India

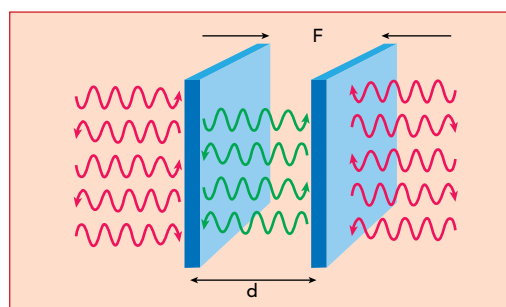
Ajay K. Poddar and Ulrich L. Rohde
Synergy Microwave, N.J., U.S.

MEMS switches offer inexpensive, high performance solutions but reliability issues arising from stiction in MEMS switching devices can exclude the technology for high frequency applications.¹⁻⁹ In this article, a new MEMS Switch is reported using an artificial composite structure (or metamaterial) which can produce a repulsive Casimir force between metal and metamaterial structure realized by a high conductivity material.²⁻⁵ This approach can resolve the stickiness problem, leading to new fabrication methods in next generation electro-mechanics linked to 5G and IoT applications.

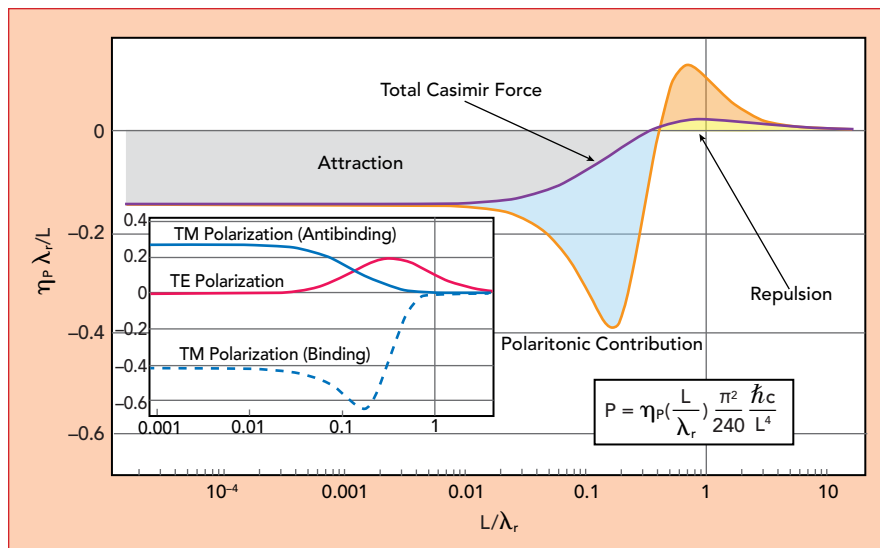
CASIMIR EFFECT

The Casimir force originates from the interaction of surfaces with the surrounding electromagnetic spectrum and exhibits a dependence on the dielectric properties of the surfaces and the medium between the surfaces. Casimir forces between macro-

scopic surfaces have the same physical origin as atomic surface interactions and those between two atoms or molecules (van de Waals forces) because they originate from quantum fluctuations. In the case of two uncharged metal plates positioned closely to one another and in parallel, a force causing the two plates to move towards one another has been observed.³ **Figure 1** shows the Casimir force 'F' on parallel plates kept in



▲ **Fig. 1** Casimir force 'F' on parallel plate kept in vacuum.³

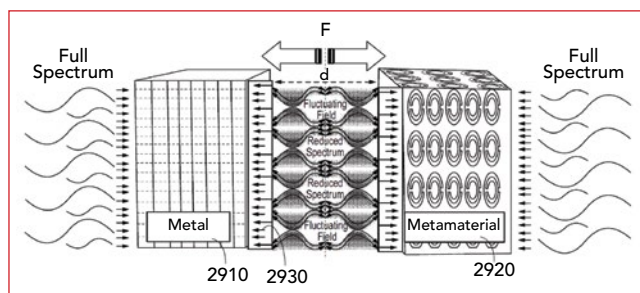


▲ Fig. 2 Plots show the region of Casimir Force of attraction and repulsion.⁴

vacuum. The effective force is $F \propto A/d^4$, where A is the area of plate and d is the distance between the plates.³

The Casimir force is proportional to the effective permittivity of metal plates.^{3,4} Therefore, by decreasing the effective permittivity on the metal planes, the Casimir force can be decreased. This can result in reduced forces preventing the plates from separating from one another, thus at least partially mitigating the stiction problem observed in MEMS switches.² Figure 2 shows the polaritonic characteristics of the Casimir force of interaction that includes attraction and repulsion.⁴

It is possible to reduce the likelihood of stiction by increasing the bias voltage applied to the switch as discussed in Part I of this article series (May issue). Alternatively, the electric field of the switch can be increased by distancing the top electrode from ground.⁶ This can be accomplished, for example, by sandwiching the conductive layer (e.g., gold) between two dielectric layers (e.g., silicon oxynitride). Another alternative is to modify the beam to maximize its restoring force without having to increase the bias voltage. Increased restoring force is influenced by parameters such as in-



▲ Fig. 3 Demonstration of the Casimir force in metamaterial structure.²⁻⁵

creased plate size, shortened beam length or increased dielectric thickness. In addition to controlling the distance between the electrode and ground, and controlling the structural parameters of the switch contacts, it is also proposed in this article to weaken or reverse the forces applied to the switch contacts due to their proximity.

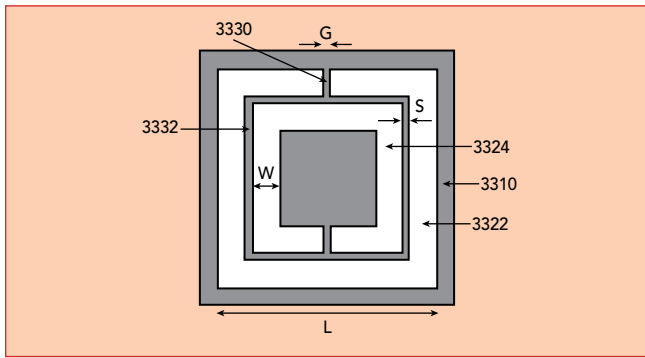
APPLICATION OF CASIMIR EFFECT IN MEMS SWITCHES

By reducing permittivity between plates, a repulsive force can be produced if the effective permittivity is sufficiently decreased, such as by engineered materials known as metamaterials.⁷ Thus, generating a repulsive Casimir force can result in even less of a liability for the contacts to become “welded” together due to stiction. Figures 3 and 4 illustrate the repulsive force, described as Casimir effect.¹⁻⁸ Figure 3 is a force diagram of an experimental setup, in which a plane of metal (2910) is positioned in par-

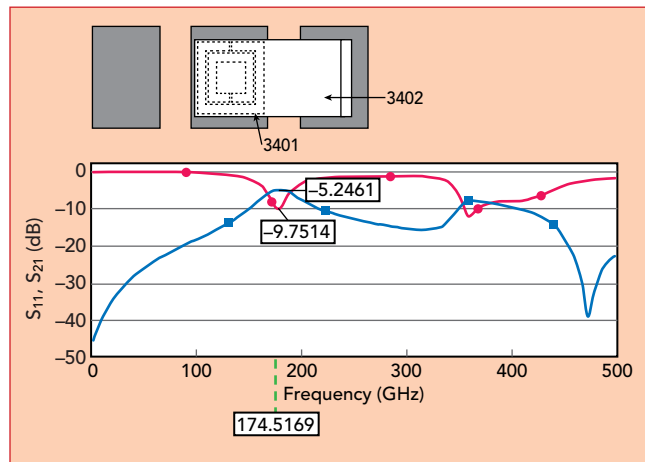
allel to a metamaterial (2920). The metal and metamaterial are positioned apart from one another at a distance “ d .” The forces illustrated in the setup in Figure 3 are shown using arrows (2930). A force applied to the metal and metamaterial bring the two planes closer to one another. However, application of this force has been observed under the specific conditions of the experimental setup illustrated in Figure 4 to result in a second and opposite force “ F ” that causes the two planes to separate from one another. Figure 4 shows a typical example of a levitating mirror.⁵ The repulsive Casimir force of the metamaterial may balance the weight of one of the mirrors, letting it levitate on the zero-point fluctuation.

Figure 4a shows a first metal plate (3010) or mirror separated from a second metal plate (3040) or mirror by a distance “ d .” The two metal plates may be thought of as opposing contacts in a MEMS switch, and may be liable to become permanently stuck to one another at distances “ d ” that are sufficiently small. By contrast, Figure 4b shows a thin layer of metamaterial (3020) affixed to a surface of the first metal plate (3010) and positioned in between the metal plates (3010, 3040). A Casimir force (3030) is produced at the boundary between the metamaterial (3020) and the second metal plate (3040), thereby causing the second metal plate to further separate from the first metal plate by a distance “ d .” This additional separation may even counteract gravitational forces, and thus cause the second metal plate to levitate. As an example, the metamaterial could be made by split ring structure using gold foil.⁴⁻⁷

In the application of a MEMS switch structure, the switch may include a deflectable beam having a shorting bar positioned on a surface of the beam and aligned with the contact of the signal line. The shorting bar may be made of metal, such as a thin layer of gold foil. When the shorting bar touches the signal line, the metal-to-metal contact surfaces may stick to one another in the form of strong adhesion. This adhesion causes undesirable stiction problems, which in turn may



▲ Fig. 7 The split ring configuration.



▲ Fig. 8 The transmission and reflection characteristics of composite structure example #1.

also include a metamaterial unit cell (3115) in order to acquire the desired permittivity.

EXAMPLE REPULSIVE CASIMIR FORCE INSPIRED RESISTIVE CONTACT MEMS SWITCH

Figure 6 shows an example MEMS switch incorporating metamaterial cells to provide a repulsive Casimir force between contacts of the switch. This metamaterial inspired MEMS switch is formed in a coplanar waveguide (3201) having two ground planes (3202 and 3204) formed above a substrate (3205). The ground planes are separated by a channel and a signal line (3210) that is formed lengthwise in the channel. The signal line includes an input port (3212) through which a signal is received (arrow in) and an output port through which the signal is transmitted (arrow out).

This MEMS switch includes a cantilevered beam that moves in and out of the plane of the coplanar waveguide in order to move in and out of contact with the signal line. The beam includes multiple layers. In Figure 6, from top to bottom, the layers include: a top layer (3420) of dielectric material, a first metal layer (3210), a dielectric layer (3220) and a second metal layer (3230). Each of the first and second metal layers may include a metamaterial device (3215 and 3235) encased within, as shown in the cross-sectional view of Figure 6c.

The top layer (3210) and first metal layer (3220) may be adapted to extend across the entire length of the beam, whereas the length of the sandwiched dielectric layer (3220) and second metal layer (3230) may be

limited to the area above the signal line. Alternatively, the dielectric layer may extend the entire length of the beam while only the second metal layer may be limited to the area above the signal line (3210). The ground planes (3202 and 3204) and signal line ports (3212 and 3214) may be separated from the substrate (3205) by a thin layer of dielectric (3250), such as SiN or SiO₂.

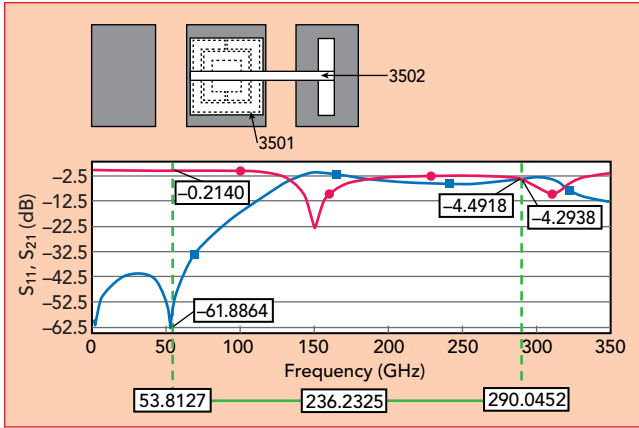
Operation of the switch may be controlled by moving an anchor (3270) to which the beam is attached in and out of the plane of the coplanar waveguide (3201). In this case, the ground line (3202) may include a hole (3260) through which a post or anchor (3270) of the beam is positioned. Moving the post up and down can result in the contacts of the switch separating or contacting one another, respectively. Figure 6d shows the switch closed, with the contacts contacting one another.

In the example of Figure 6, the section of the coplanar waveguide shown may be about 100 μm, and the beam may have a width of about 75 μm. The anchor to which the beam is attached may have a length (in the direction of the beam length) of about 11.25 μm and a width of about 75 μm. The opening into which the beam is anchored may have a greater length and width, such as about 80 × 30 μm. The overall length of the waveguide (in the direction of the beam length) may be about 330 μm, whereby the ground planes and the signal lines may each have a width (also in the direction of the beam length) of about 75 μm, with 38 μm channels in between. The beam may have a length of about 140 μm (not including the length of the anchor).

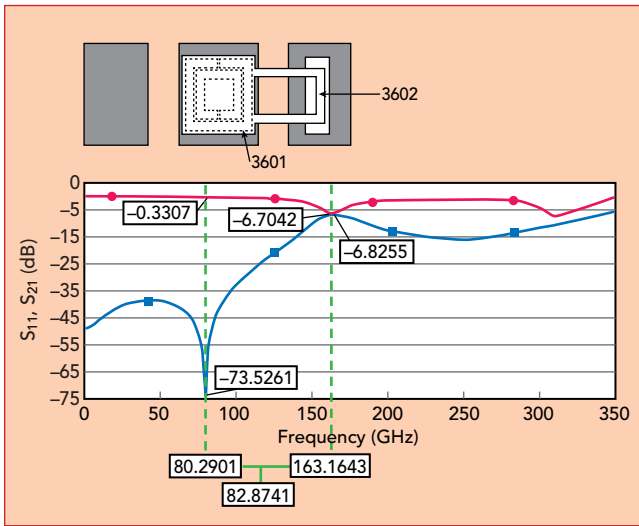
The overall height of the beam when in the closed position may be about 5 μm, relative to the dielectric surface on which the ground planes and signal line are formed. Each of the ground planes and signal line may be 2 μm thick. The beam may then contribute an additional 3 μm to the height of the switch, whereby each of the metal layers (3210 and 3230) is about 1 μm thick and the dielectric layer sandwiched in between may also be about 1 μm. The top layer (3440) may add about 0.2 μm to the height of the switch. The metamaterial unit cells made of split rings²⁻⁷ included in the second metal layer (3230) and optionally in the first metal layer (3210).

Figure 7 illustrates an example, the metal layer (3310) with a first split ring (3322) having width L, and a second split ring (3324), formed in the layer (forming the rings may involve cutting out the rings from the layer). Each of the rings may be concentric and aligned so that the splits (3330) in the respective rings are positioned on opposing sides of the layer (3310). Each of the rings may have a uniform width W, and the splits may have a uniform width G. The rings may further be separated from one another by a uniform separation (3332) having width S. Different engineered structures may provide different metamaterial unit cells that can exhibit characteristics at the relevant band of frequencies for MEMS switch.¹⁻²

Figures 8-10 show test results for transmission and reflection characteristics for a respective unit cell structure. The metamaterial cell shown in Figure 8 is included in a metal layer having a width equal to the width of the beam (3402). In this example, the unit cell is of transmission type at low frequencies, at about 300 GHz



▲ Fig. 9 The transmission and reflection characteristics of composite structure example #2.

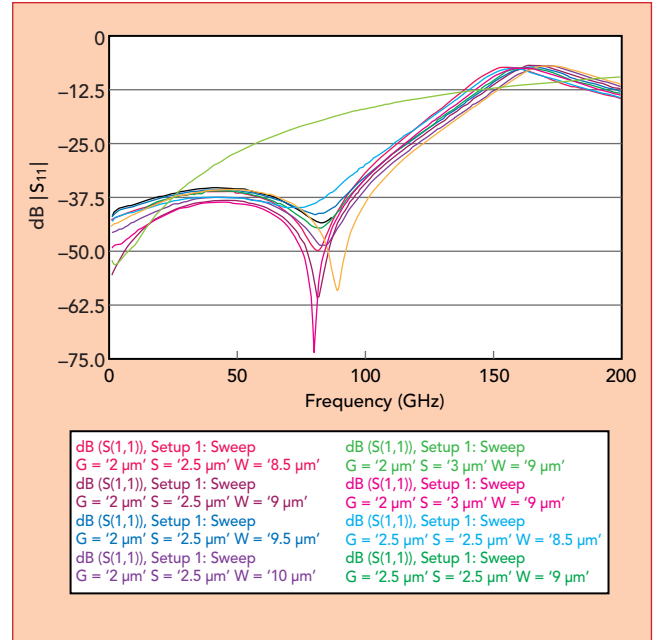


▲ Fig. 10 The transmission and reflection characteristics of composite structure example #3.

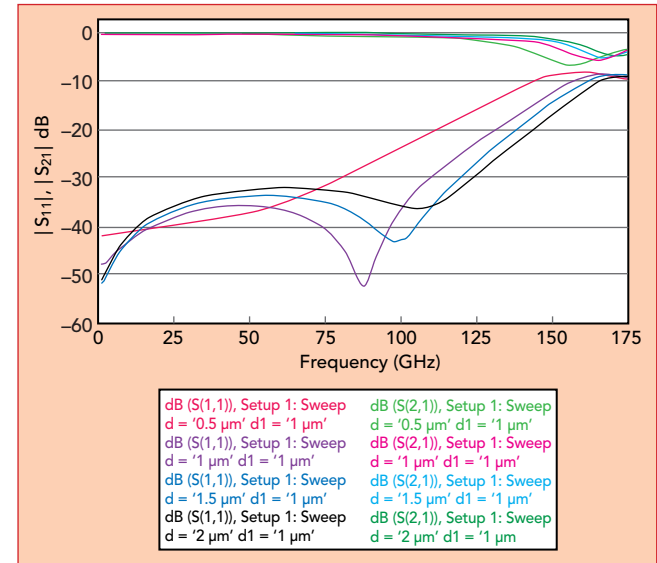
and again at about 470 GHz. The unit cell is of reflection type, with attenuation of the transmission exceeding that of the reflection, at about 150 GHz and again at about 300 GHz. Thus, the composite structure of Figure 8 is shown to exhibit metamaterial properties.

The composite structure (3501) shown in Figure 9 is included in a metal layer having a length equal to the width of the signal line, and further attached to a beam (3502) having a width much smaller than the width of the metal layer. In this example, the unit cell is shown to have transmission properties at about 54 GHz and reflection properties at about 150 GHz. Therefore, the composite structure of Figure 9 is also shown to exhibit metamaterial properties.

The composite structure (3601) of Figure 10 is included in a metal layer having a length equal to the width of the signal line, and further attached to a U-shaped beam (3602) having two branches each having width much smaller than the width of the metal layer. In this example, the unit cell is shown to have transmission properties at about 80 GHz and reflection properties at about 163 GHz. Therefore, the structure of Figure 10 is also shown to exhibit metamaterial properties, and these properties can be exhibited over a relatively nar-



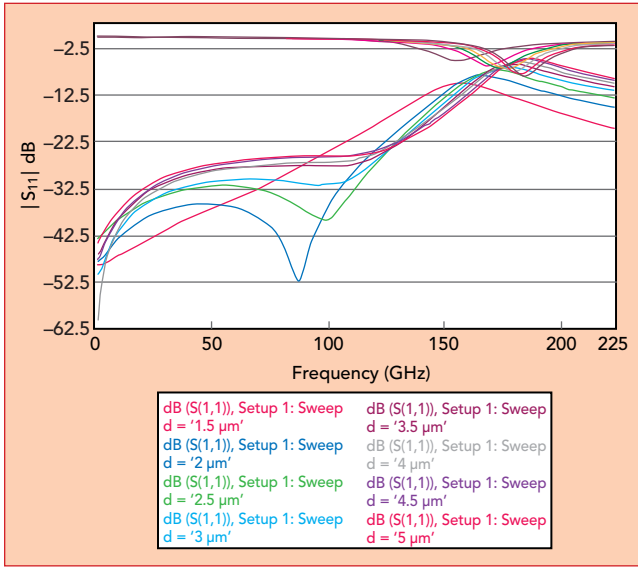
▲ Fig. 11 Shows plots of reflection characteristics for a metamaterial cell with varying parameters G, S and W, given in Figure 7.



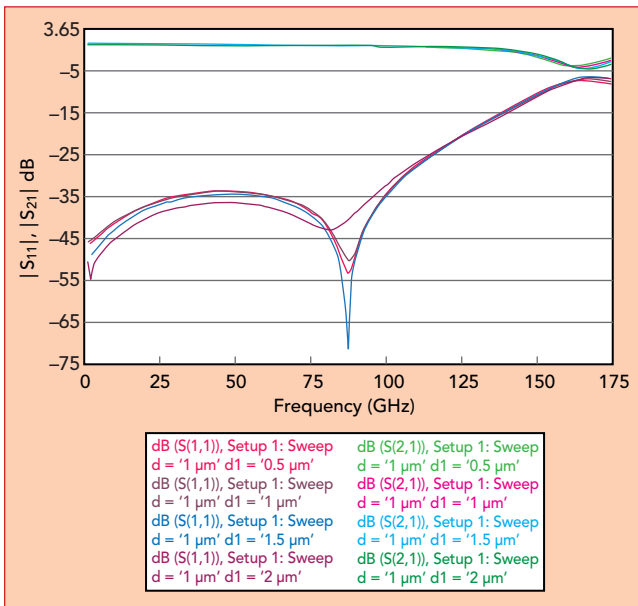
▲ Fig. 12 Shows plots of transmission and reflection characteristics of a switch for which the thickness of the second metal layer "d" (e.g., 3230 of Figure 6 varies between 0.5 μm through 2 μm).

row bandwidth of about 80 GHz.

Additionally, the parameters of the metamaterial cell structures can be varied to produce different transmission and reflection characteristics. For example, **Figure 11** provides a graph plotting reflection characteristic for a metamaterial cell having different parameters G, S and W (as defined in Figure 7). In Figure 11, it can be seen that the frequency at which reflection is most greatly attenuated, varied from about 80 to 90 GHz depending on G, S and W. For instance, where G is 2 μm, S is 3 μm and W is 9 μm, insertion loss drops to about 74 dB at 80 GHz. By comparison, other parameters of G, S and W yield a reflection of about -60 dB at about 90 GHz.



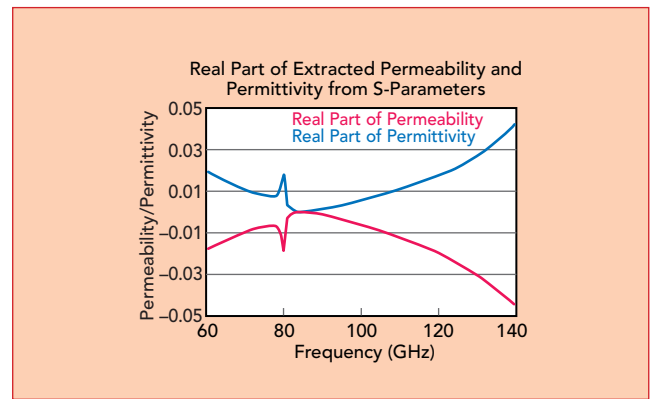
▲ Fig. 13 Shows plots of transmission and reflection characteristics of a switch for which the thickness of the second metal layer “d” (e.g., 3230 of Figure 6 varies between 1.5 μm through 5 μm).



▲ Fig. 14 Shows the plot of transmission and reflection properties of a switch for which the thickness of the first metal layer “d1” (e.g., 3210 of Figs. 6 varies between 0.5 μm through 2 μm).

In addition to the use of variation of composite structure for the realization of metamaterial cell and cell structure parameters, the metal layers of the MEMS switch may also be formed with different parameters and dimensions as compared to those parameters and dimensions.

Figure 12 is a plot of both transmission and reflection properties of a switch where the thickness of the second metal layer “d” (e.g., 3230 of Figure 6) varies between 0.5 μm and 2 μm. Figure 13 is a plot of transmission and reflection properties of a switch where the thickness of the sandwiched dielectric layer (e.g., 3220 of Fig. 6) varies between 1.5 μm and 5 μm. Figure 14 is a plot of transmission and reflection properties of a switch where the



▲ Fig. 15 Shows the plot of permittivity extracted from the S-parameters of the composite structure in Figure 6.

thickness of the first metal layer “d1” (e.g., 3210 of Fig. 6) varies between 0.5 μm and 2 μm. The transmission properties of the various MEMS switches are largely similar in each of these conditions, although the frequency at which the transmission attenuates varies between about 160 and 180 GHz, and the reflection properties of the switch vary mainly between 60 and 150 GHz.

Using the transmission and reflection data, permeability and permittivity of the metamaterial cells can be extracted using parameter extraction procedures.⁶ The parameter extraction is shown in Figure 15. The composite structure exhibits near zero permittivity and permeability at a band of frequencies centered around 85 GHz. Therefore, these structures would produce a repulsive Casimir force around the band of frequencies ranging from about 60 to 130 GHz.

Figures 16 and 17 further demonstrate the overall response of the MEMS switch in each of its ON and OFF states, respectively. In Figure 16, when the switch is OFF, and thus not passing the transmitted signal between input and output ports, the reflection characteristics are shown to be just slightly less than 0 dB even at frequencies of up to 130 GHz, the transmission characteristics are between about -20 dB and -15 dB between operating frequencies of about 60 to 130 GHz. In Figure 17, when the switch is ON, and thus passing the transmitted signal between input and output ports, the reflection characteristics are as low as about -73.5 dB at 80 GHz with the transmission characteristics as high as -0.33 dB while the reflection and transmission characteristics at 163 GHz are both about -6.75 dB.

The examples of Figures 6 through 17 demonstrate the possibility of incorporating metamaterial structures into a high frequency resistive MEMS switch in order to reduce the effects of stiction.¹⁻²

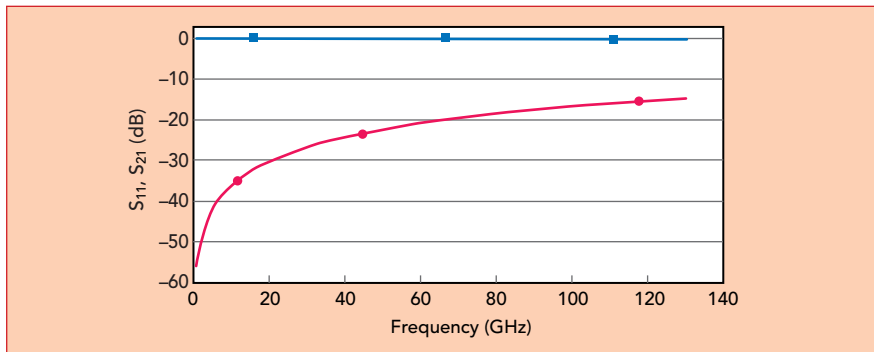
CONCLUSION

In this article (Part II), the principle of repulsive Casimir force is applied to improve stiction of the resistive contact MEMS switch. This approach can be similarly applied to capacitive contact MEMS switches. As with the resistive switch, a sandwich of metal and dielectric layers used to achieve the desired permittivity interface, such as having a gold layer with infinite permittivity, a dielectric layer with positive but low permittivity and a metamaterial

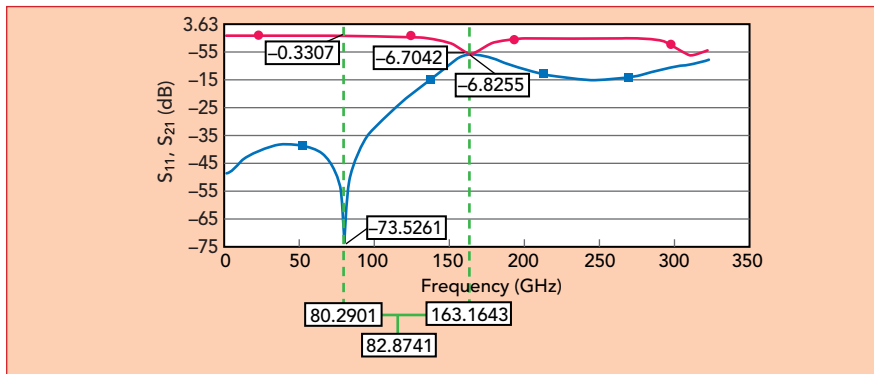
Technical Feature

layer with a permittivity in the range of about zero or less. Unlike the example switches here, in the capacitive switch, the metamaterial layer can be

used as part of the signal line contact instead of as part of the beam contact and will be covered in Part III (coming in the July issue). ■



▲ Fig. 16 Response of the MEMS switch.



▲ Fig. 17 Response of the MEMS switch.

References

1. Shibani Koul, Chaitanya Mahajan, Ajay Poddar and Ulrich Rohde, "A Microelectromechanical Switch with Metamaterial Contacts, Part I: Concepts and Technology," *Microwave Journal*, pp. 82-108, May 2020.
2. Shibani Koul, Ajay Poddar and Ulrich Rohde, "Microelectromechanical Switch with Metamaterial Contacts," US Patent Pub. No. 02161415A1.
3. Astrid Lambrecht, "The Casimir Effect: A Force from Nothing," *Physics World*, September 2002.
4. F. Intravaia and C. Henkel, *New Frontiers of Casimir Force*, Santa Fe, New Mexico, 2009.
5. U. Leonhardt and T. G. Philbin, "Quantum Levitation by Left-Handed Metamaterials," *New J. of Physics*, August 2007.
6. Mercado et. al., "A Mechanical Approach to Overcome RF MEMS Switch-Stiction Problem," ECTC 2003.
7. Ulrich Rohde, Ajay Poddar and Shibani Koul, "MTM: Casimir Effect and Gravity Wave Detection," APMC 2016.
8. Xudong Chen et.al, Robust Method to Retrieve the Constitutive Effective Parameters of Metamaterials, *Phy. Rev. E* 70, 016608, July 2004.
9. Chaitanya Mahajan, Design and Analysis of RF MEMS switches (70 GHz to 130 GHz), M.Tech Dissertation, CARE, IIT Delhi, May 2018.